J Appl Electrochem (2008) 38:315–320
DOI 10.1007/s10800-007-9440-z

ORIGINAL PAPER

Initial stages of nucleation of molybdenum and tungsten carbide phases in tungstate–molybdate–carbonate melts

V. Malyshev · A. Gab · M. Gaune-Escard

Received: 16 June 2005 / Revised: 26 October 2007 / Accepted: 30 October 2007 / Published online: 23 November 2007

Abstract The electrochemical nucleation of Mo_2C and W_2C crystals for tungstate–molybdate–carbonate melts of specific compositions on Ag, Au, Cu, Pt, and Ni substrates was studied by the electrodeposition method. The influence of electrocrystallization conditions (temperature, deposition time, initial current pulse, and current density) was investigated. Experimental measurements indicate that crystallization overvoltage is associated with three-dimensional nucleation. Carbide deposition onto the substrates prepared from the same solid materials was not associated with crystallization overvoltage. The maximum value of the initial overvoltage, η_{max}, which includes crystallization and electrolysis overvoltages, is proportional to the electrode surface area. Under these conditions, surface diffusion limits the electrode process rate. An increase in carbide deposition rate leads to an increase in the number of crystallization centers. This reduces the duration of surface diffusion. A rise in the melt temperature complicates the crystallization process by alloy-formation phenomena. Overvoltage maximum height for metals, which do not form alloys, is proportional to the reciprocal of their formation time. Melt temperature increase promotes interdiffusion of refractory metal, carbon, and substrate, and also intensifies their chemical interaction. Structural mismatch is observed during molybdenum and tungsten carbide electrodeposition onto different single-crystal substrates.

Keywords Crystallization overvoltage · Electrolysis · Ionic melt · Molybdenum carbide · Nucleation · Tungsten carbide

1 Introduction

Usually, Mo, W, Mo_2C, and W_2C coatings are deposited onto non-oriented metal substrates by electrolysis of Na_2WO_4-based oxide melts [1–4]. However, in many instances it is necessary to obtain continuous cathode deposits with preset properties (structure, orientation, and crystallite size). Therefore, an important role in electrolysis is played by the initial stages of crystal nucleation. The results of related investigations for electrodeposited Mo and W were presented earlier [5–7]. The initial stages of Mo and W carbide nucleation have not been studied so far. The only known study was performed for platinum and glassy carbon electrodes [8]. The present work was undertaken to study initial nucleation stages of carbide phase crystals in oxide melts on various metallic substrates under different electrodeposition conditions.

2 Experimental methods

The initial stages of crystal nucleation were investigated by electrochemical methods suitable for phase formation study with simultaneous microstructural investigation of substrate surface and electrolysis products. The experimental installation consisted of a stainless steel reactor inside a resistance furnace; an analytical radiometer

V. Malyshev (✉) · A. Gab
National Technical University of Ukraine "Kyiv Politechnic Institute", Peremoha ave 37, Kyiv 56 03056, Ukraine
e-mail: victor_malyshev@mail.ru

M. Gaune-Escard
Ecole Polytechnique Universitaire de Marseille, IUSTI-UMR CNRS 6595 Technopole de Château-Gombert, 5 Rue Enrico Fermi, 1345 Marseille Cedex 13, France
e-mail: Marcelle.Gaune-Escard@polytech.univ-mrs.fr

(Voltalab PST 050) was used for measuring potential–time curves, i.e., time dependence of electrode potential in galvanostatic electrolysis. Microstructural studies were performed with a MBS-9 microscope. Measurements were performed in a three-electrode cell. The anode was a platinum crucible, which was simultaneously used as melt container. The working electrode was a metal wire (Ag, Au, or Cu) 0.5–10 mm wide sealed into one end of a quartz tube and polished. The reference electrode was a Mo_2C or W_2C strip pressed onto platinum current leads. These electrodes were in equilibrium state with melts used for carbide electrodeposition and therefore their electrode potential can be conventionally assumed to be equal to zero. After being washed with distilled water, deposits were studied with a DRON-4 X-ray diffractometer and a Stereoscan S-4 scanning electron microscope. Grain size was averaged over 50–100 crystals. Surface morphology of layers was determined with a Camebax scanning electron microscope.

3 Results and discussion

Study of the initial stages of molybdenum carbide nucleation was carried out in melts of the following compositions: Na_2WO_4—1 mol.% MoO_3 (under CO_2 pressure) and Na_2WO_4—5 mol.% MoO_3—10 mol.% Li_2CO_3. Investigation of tungsten carbide nucleation was realized in melts of the following compositions: Na_2WO_4—1.5 mol.% WO_3 (under CO_2 pressure) and Na_2WO_4—10 mol.% WO_3—15 mol.% Li_2CO_3. Electrolysis products in these melts were Mo_2C and W_2C as confirmed by X-ray phase analysis. As shown earlier [5, 7], carbide electrodes in tungstate–molybdate–carbonate melts of different composition show thermodynamically determined equilibrium electrode potentials. These results were also confirmed by a kinetic study of carbide coating electrodeposition onto solid electrodes. Charge–discharge curves were obtained by measurement of electrode potential changes versus time with superposition of current impulses of certain amplitude and duration, which are selected experimentally. Amplitude values reached overvoltage peak. The impulse duration allowed us to attain the equilibrium electrode potential value. Time dependence of electrode potential versus the reference platinum–oxygen electrode is shown in Fig. 1. In this figure, the right-hand ordinate overvoltage scale η relative to equilibrium potential E_{eq}, taken as zero, visualizes crystallization overvoltage η_{cr} as the difference between the electrode potentials at points A and B. The left-hand ordinates correspond to the Pt reference electrode, which is necessary for comparison of Pt and carbide reference electrodes under excessive CO_2 pressure. As can be seen from the

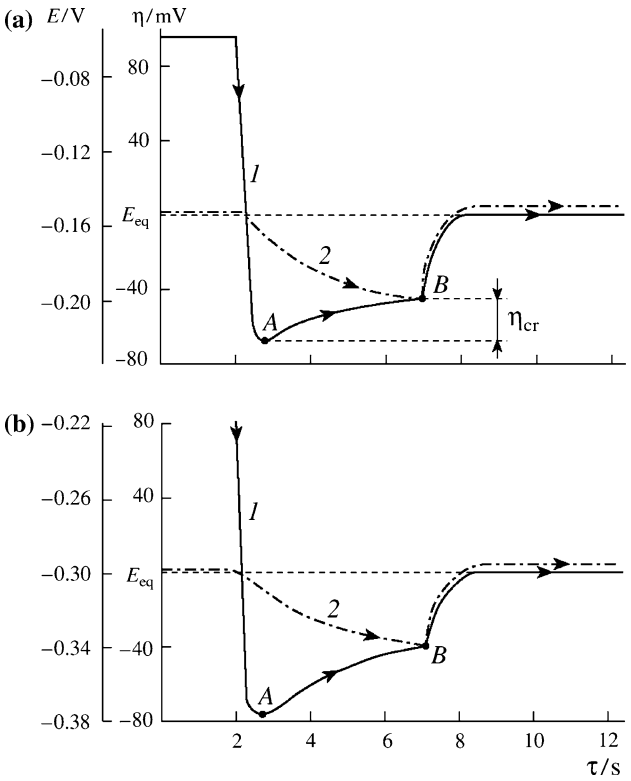

Fig. 1 Charge–discharge curves of (**a**) Mo_2C and (**b**) W_2C electrocrystallization on electrodes prepared from (1) Ag, (**a**, curve 2) Mo_2C, and (**b**, curve 2) W_2C (2) $T = 1{,}073$ K; cathode area 7.5×10^{-3} cm^2. (**a**) Na_2WO_4 melt—1 mol.% MoO_3 at 7.5 atm. CO_2, $i_{pulse} = 0.75$ mA; $\tau_{pulse} = 5$ s. (**b**) Na_2WO_4–1.5 mol.% WO_3 melt at 10 atm. CO_2, $i_{pulse} = 1.0$ mA; $\tau_{pulse} = 5$ s

charge–discharge curves in Fig. 1, deposition of carbide onto a solid foreign substrate with current onset is characterized by three important features (Fig. 1, curve 1): the negative potential shift (point A), the positive potential shift until reaching a steady state, and the equilibrium potential value of deposited compound after current offset (point B).

It is established that the first crystals start growing immediately after the appearance of the current peak of the charge–discharge curves. Repeated current impulse within short time periods (5–10 s) does not induce peak formation. These facts confirmed three-dimensional nucleation. From the results, the crystallization overvoltage due to the considerable energy consumption for component nucleation in the initial stages of synthesis was evaluated. These overvoltages at Ag electrodes range between 8 and 20 mV within the temperature range 973–1,023 K. Carbide deposition onto the substrate prepared from the same solid material was not associated with crystallization overvoltage (Fig. 1, curve 2). That is why the current is zero at point A. The maximum value of initial overvoltage η_{max}, which includes crystallization and electrolysis overvoltages, is proportional to the electrode surface area (Fig. 2) for

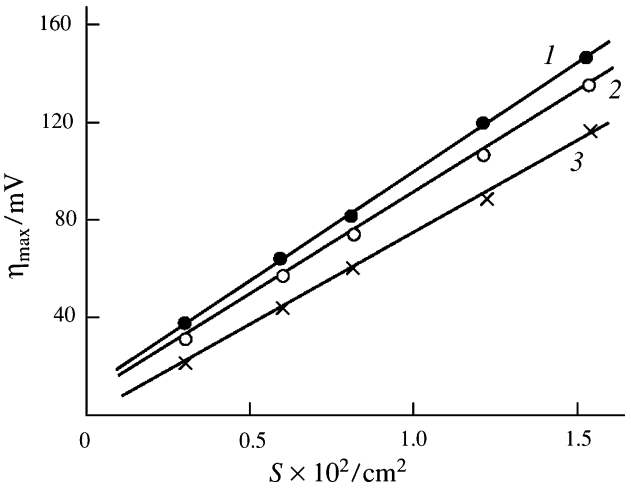

Fig. 2 Electrode area S influence onto η_{max} value during electrodeposition of W_2C ($T = 1{,}173$ K, $i = 0.1$ A cm^{-2}) onto various electrodes ((1) Ag, (2) Au, and (3) Cu) in Na_2WO_4—10 mol.% WO_3—15 mol.% Li_2CO_3 melt

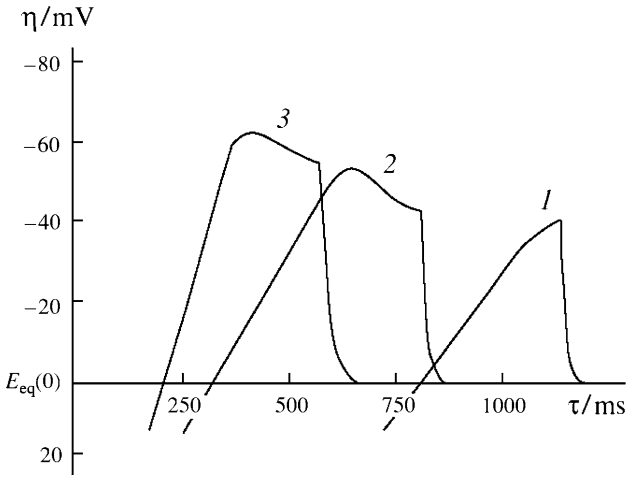

Fig. 4 Charge–discharge curves of W_2C electrocrystallization at Ni electrodes (1) without oxide film and (2, 3) with oxide film in Na_2WO_4—10 mol.% WO_3—15 mol.% Li_2CO_3 melt. Oxidation time of Ni in air at $T = 1{,}273$ K is (2) 15 and (3) 30 min

electrodes, which do not form alloys with W. Under these conditions, surface diffusion limits the electrode process rate. The number of crystallization centers increases with the carbide deposition rate. As a result, the surface diffusion rate exceeds the electron transfer rate or the electroactive species diffusion rate from melt bulk. Thus, higher overvoltages seem to change limiting step so that the process rate is determined either by the electron transfer rate or by the rate of diffusion from the melt.

An increase in melt temperature may complicate the crystallization process due to the interaction between the deposited components and the matrix material (Fig. 3). For example, during Mo_2C electrodeposition onto a Pt

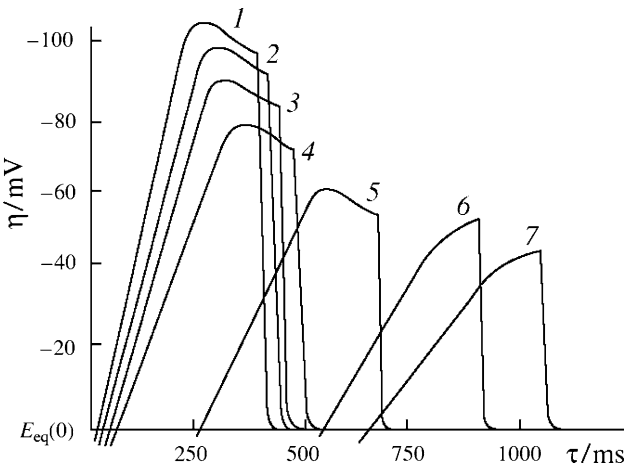

Fig. 3 Charge–discharge curves of Mo_2C electrocrystallization at Pt electrode at various melt temperatures ($S = 7.5 \times 10^{-3}$ cm^2, $i_{pulse} = 0.75$ mA and T equal to (1) 1,023; (2) 1,053; (3) 1,083; (4) 1,103; (5) 1,123; (6) 1,173; and (7) 1,223 K) in Na_2WO_4—5 mol.% MoO_3—10 mol.% Li_2CO_3 melt

electrode, the overvoltage (difference between peak potential and equilibrium potential) decreases from 100 mV at 1,023 K to 60 mV at 1,123 K. During further temperature increases, there are no overvoltage peaks, which is probably connected with the initiation of Mo interaction with Pt. For metals forming alloys with deposited components, crystallization overvoltage is observed for the surface oxide film (Fig. 4). With Ni electrodes, previously oxidized in air, overvoltage is observed (Fig. 4, curves 2 and 3). With increase of oxidation time, overvoltage increases. This is probably associated with surface oxide layer interference with Ni–W alloy formation. After mechanical surface treatment, each working electrode was electrochemically polished with simultaneous microscopic control of substrate state. Electrochemical polishing time was determined with allowance made for the time of disappearance of the layer of metal disturbed by mechanical surface treatment [9]. Mechanical processing promoted oxide film removal from the electrode surface, and there was no overvoltage at the electrode after such processing (Fig. 4, curve 1).

A typical charge–discharge curve corresponding to carbide electrodeposition onto native substrate over wide temperature (973–1,173 K) and current density ($i = 0.02$–0.40 A cm^{-2}) ranges indicates absence of any crystallization hindrance and of any passivating surface films (Fig. 5). Neither increase in temperature nor current density leads to the appearance of an overvoltage peak. To determine the inertness of the substrate, overvoltage maximum values and appearance times were studied during electrocrystallization of Mo_2C under galvanostatic conditions at Mo, Ti, Ni, Ag, Cu, Pt, and Mo_2C substrates. The choice of working electrode material was made with due regard for

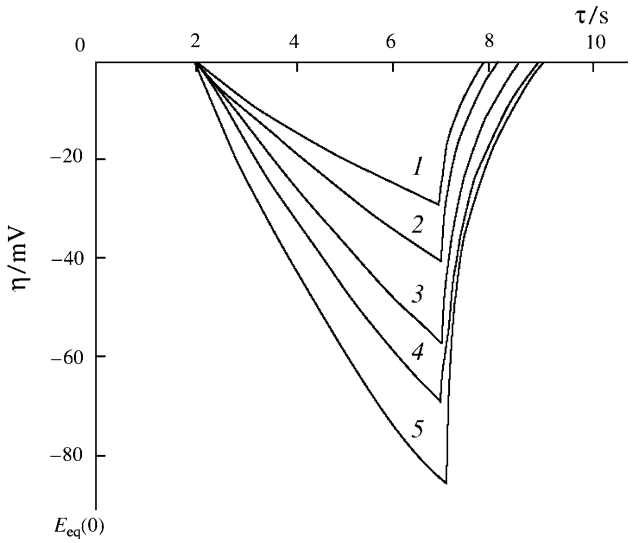

Fig. 5 Charge–discharge curves of Mo_2C electrocrystallization at native substrate ($S = 7.5 \times 10^{-3}$ cm^2, $\tau_{pulse} = 5$ s) from Na_2WO_4—5 mol.% MoO_3—10 mol.% Li_2CO_3 melt at the following values of T, K and i_{pulse}, mA: (1) 973, 0.37; (2) 1,173, 0.75; (3) 1,073, 0.75; (4) 973, 0.75; (5) 973, 2.25

its diffusion properties [10] and for its binary phase diagrams with Mo or C [11]. Figure 6 shows charge-discharge curves obtained at $T = 1{,}173$ K with current density $i = 0.14$ A cm^{-2}. These curves reflect the initial stages of Mo_2C electrocrystallization at various substrates. Obviously, under such conditions, Ag, Au, and Cu do not form alloys with W as shown by the overvoltage peak (see Fig. 6, curves 1–3). In contrast, Pt and Ni do form such alloys as indicated by the presence of the overvoltage peak (see Fig. 6, curves 4 and 5).

It is characteristic that the overvoltage maximum height for the abovementioned metals is proportional to formation time. For example, Table 1 shows the overvoltage peak

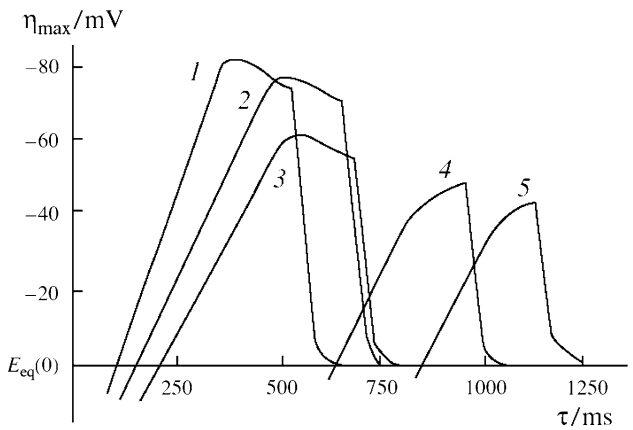

Fig. 6 Charge–discharge curves of W_2C crystallization at substrates made from different materials ($S = 7.5 \times 10^{-3}$ cm^2, $i_{pulse} = 0.75$ mA, $T = 1{,}173$ K; (1) Ag, (2) Au, (3) Cu, (4) Pt, and (5) Ni) in Na_2WO_4—10 mol.% WO_3—15 mol.% Li_2CO_3 melt

Table 1 Overvoltage peaks heights (i) and their inverse times ($1/\tau$) for W_2C electrodeposition process from Na_2WO_4—1.5 mol.% WO_3 melt under 10 atm of CO_2 excessive pressure at 1,073 K within current density interval 0.03–0.20 A cm^{-2}

i (A cm^{-2})	η (mV)	$1/\tau$ (s^{-1})
0.20	112	2.5
0.15	90	1.75
0.10	77	1.32
0.07	71	1.15
0.03	64	0.97

height and the inverse values of formation times. The linear character of this dependence seems to be associated with the partial penetration of deposited components into the substrate bulk due to solid-phase diffusion. This allows qualitative characterization of the degree of inertness of the substrate material. Thus, the crystallization overvoltage η_{max} for the Ni substrate is observed only at certain current densities. At Pt, noticeable depolarization is observed with two pronounced waves, which correspond to the formation of alloys with different compositions.

Usually, increase in melt temperature activates the cathode surface, increases the rate of interdiffusion of deposited material components with the substrate, and also intensifies the chemical interaction between them. It has been shown experimentally that Mo_2C electrodeposition at temperatures above 1,173 K, even in the case of inert Ag substrate, is accompanied by depolarization due to alloy formation. Measurements over a wide temperature range (973–1,123 K) indicate that the initial stages of Mo_2C electrocrystallization at the substrate surface vary with temperature. Figure 7 shows charge–discharge curves reflecting the nucleation of a new phase at each temperature. Curves 1–3 clearly demonstrate that the critical energy for the formation of nuclei decreases. Conversely, more time is required to achieve a degree of saturation by adatoms sufficient for new-phase formation. A temperature rise up to 1,223 K removes crystallization hindrances for new phase formation consisting of stable aggregates. Further temperature increase results in the stable appearance of intensive depolarization processes due to new phase growth.

Figure 8 shows the dependence of Ag electrode potential on time during the electrodeposition of Mo_2C. It indicates that crystallization overvoltage increases with current density. According to [7], if the limiting stage is the primary formation of three-dimensional nuclei, then the following relationship should hold:

$$\lg\tau = A + (K/\eta^2),$$

where τ is the time required for three-dimensional nuclei formation, A and K are constants dependent on electrode

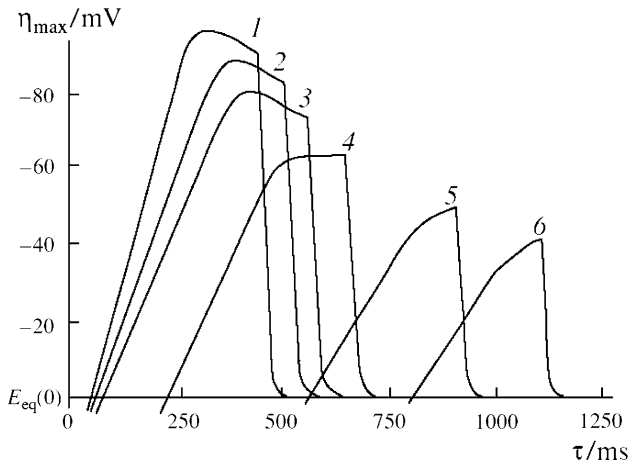

Fig. 7 Charge–discharge curves of Mo_2C electrocrystallization at Ag electrode at different temperatures ($S = 7.5 \times 10^{-3}$ cm^2, $i_{pulse} =$ 0.75 mA) in Na_2WO_4—5 mol.% MoO_3—10 mol.% Li_2CO_3 melt. $T =$ (1) 1,073; (2) 1,123; (3) 1,173; (4) 1,223; (5) 1,273; (6) 1,323 K

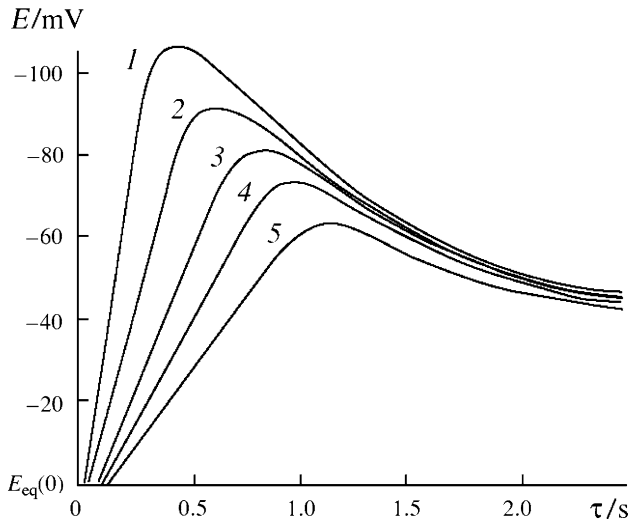

Fig. 8 Potential of Ag electrode as function of time during W_2C electrodeposition from Na_2WO_4—1.5 mol.% WO_3 melt under 10 atm. CO_2 at 1,073 K ($S = 7.5 \times 10^{-3}$ cm^2, $i_{pulse} = 1.9$ mA) at different current densities i: (1) 0.20; (2) 0.15; (3) 0.10; (4) 0.07; (5) 0.03 A cm^{-2}

material, and η is the crystallization overvoltage. It is clear from Fig. 9 that experimental points in $\lg\tau - 1/\eta^2$ coordinates fit straight lines at different melt temperatures. Deposit growth proceeds continuously.

Visually, coatings are light-grey fine-crystalline deposits. Micrographs of their surfaces (Fig. 10) and of coated sample cross-sections (Fig. 11) confirm their columnar structure.

By studying the electrodeposition of carbides onto different single-crystal substrates, we observed structural mismatch. Heteroepitaxial Mo_2C and W_2C layers on single-crystal Mo and W substrates of various orientations

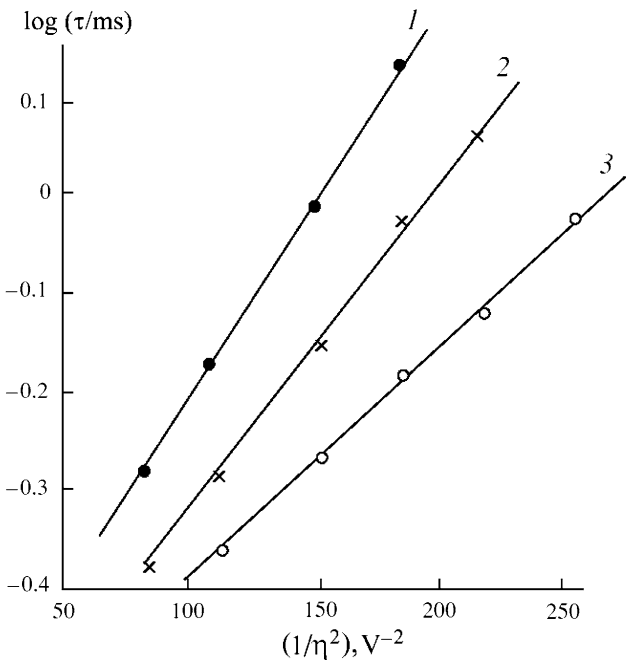

Fig. 9 Dependence of lg τ on $1/\eta^2$ during W_2C electrodeposition from Na_2WO_4—1.5 mol.% WO_3 melt at 10 atm. CO_2 at Ag electrode at the following T values: (1) 1,023; (2) 1,073; (3) 1,173 K

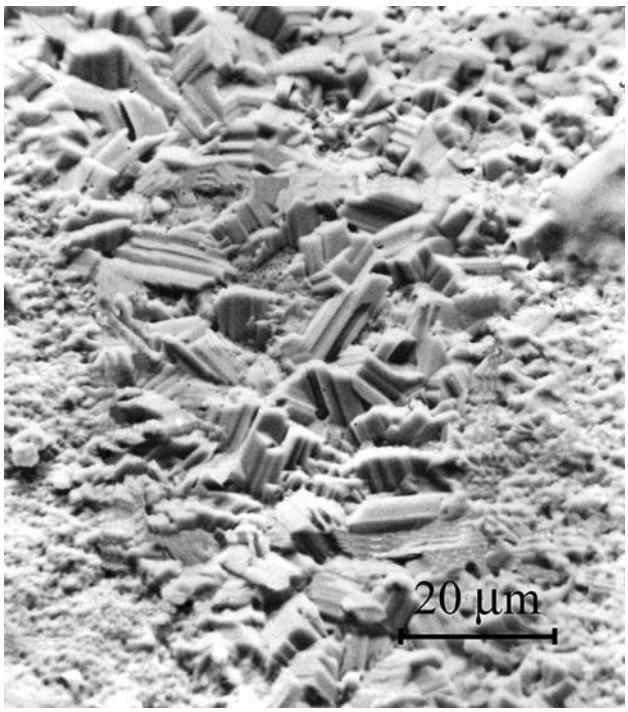

Fig. 10 Micrograph of Mo_2C coating at steel 3 surface. $T = 1173$ K; $i_k = 0.06$ A cm^{-2}; electrolysis time 1.5 h; system Na_2WO_4—5 mol.% MoO_3—10 mol.% Li_2CO_3

were deposited from the Na_2WO_4–$MoO_3(WO_3)$–CO_2 melts at $T = 1{,}123$ K and $i = (0.5–1.0) \times 10^3$ A m^{-2}. Under electrolysis conditions, using Mo substrates with {1 0 0},

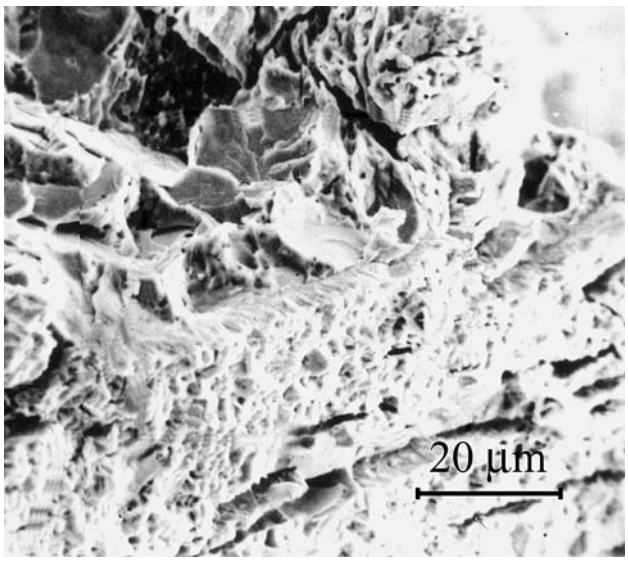

Fig. 11 Edge micrograph of steel 3 samples with Mo_2C galvanic coatings. $T = 1{,}173$ K; $i_k = 0.06$ A cm^{-2}; electrolysis time 1.5 h; system Na_2WO_4—5 mol.% MoO_3—10 mol.% Li_2CO_3

{1 1 1}, and {1 1 2} orientations and W substrates with {1 1 2} orientations, we obtained layers with one and two preferable orientations. Carbides are crystallized on these substrates as hexagonal plates differently oriented with respect to substrate surface orientation. The main faceting plane is {0 0 1}. Orientational relationships determined by X-ray diffraction analysis are the following:

$(2023)Mo_2C||(100)Mo$

$(1011)Mo_2C||(100)Mo$

$(1120)[0001]Mo_2C||(111)[112]Mo$

$(1013)W_2C||(112)W$

4 Conclusions

This experimental study of the initial stages of Mo_2C electrocrystallization from tungstate–molybdate–carbonate melts with electrodes made from various materials over a wide temperature range suggests the following concepts of nucleation. With inert substrates at $T < 1{,}073$–$1{,}173$ K, considerable crystallization hindrances are observed which are associated with three-dimensional nuclei formation. Increase in electrolysis temperature facilitates diffusion of components into the substrate, which results in a decrease in crystallization overvoltage. Transition from three- to two-dimensional nucleation also occurs. In some cases, this transition is accompanied by depolarization phenomena due to solid-phase saturation of electrode boundary layers with synthesis components (molybdenum and carbon) and to alloy formation.

Acknowledgments Most of the electrochemical work was carried out at Laboratoire IUSTI of Ecole Polytechnique Universitaire de Marseille. The authors gratefully acknowledge support within the joint Ukraine–France program "Dnipro" framework adopted between the Ministry of Education and Science of Ukraine and the French Ministry of Foreign Affairs.

References

1. White SH, Twardoch UM (1987) J Appl Electrochem 17:225
2. Takenishi H, Katagiri A (1999) Electrochemistry 67:669
3. Noel M, Syrianarayanan N (2005) J Appl Electrochem 35:49
4. Mishra B, Olson DL (2005) J Phys Chem Solids 66:396
5. Malyshev VV, Novoselova IA, Shapoval VI (1997) Molten Salts Bull 63:2
6. Kaptay G, Kuznetsov SA (1999) Plasmas Ions 2:45
7. Malyshev VV, Kushchov KhB, Shapoval VI (2002) J Appl Electrochem 32:573
8. Polischuk VA, Kushchov KhB, Shapoval VI (1990) Russ J Electrochem 26:305
9. Lovering DG (1982) Molten salt technology. Plenum Press, New York
10. Rao CNR, Gopalakrishnan J (1997) New directions in solid state chemistry. Cambridge University Press, Cambridge
11. Pearson WB (1972) Crystal chemistry and physics of metals and alloys. Wiley, New York